

Advanced Power Plant Modeling with Applications to an Advanced Boiling Water Reactor and a Heat Exchanger

Thomas D Younkins
Former Member, ASME

Prasanna Kumar Muralimanohar

Joe H Chow

2010

Advanced methods that use continuity wave equations in fluid flow paths and exact solutions of these and all other differential equations are applied to transient performance models of a counter flow heat exchanger and an Advanced Boiling Water Reactor (ABWR). The continuity wave equations for single and two-phase flow, with heat addition, are developed, and the exact solution for a typical lead lag circuit is presented. The models using these equations are described, and transient performance results are presented. These results are more accurate and are obtained with larger time intervals because of the exact solutions used. It is concluded that these two advanced methods have been successfully applied to the selected models.

1 Introduction

This paper presents two advanced modeling methods, and two applications, for power plant and component computer models, used for transient performance analysis. The methods are

1. “continuity wave” equations for the transport of thermal energy through one dimensional flow paths, with single phase flow, or two-phase flow with boiling; and with the lateral addition of heat from the wall directly or through heat transfer.
2. the exact solution of differential equations analytically first, and then the solutions put into the program; this applies to all differential equations in the program, including the continuity wave equations.

These are called “advanced” because they are so seldom used; indeed, in 38 years of advanced engineering experience, the first author has developed only one “exact solution” program and developed many other programs with numerical solutions of differential equations. Continuity wave equations may not be used, because as Graham Wallis pleaded [1, page 123], “...it is high time that the subject was given a place in elementary fluid mechanics texts”.

The advantages of these advanced methods are: greater accuracy with a simplified model; less computing time, because the exact solutions permit larger time intervals. As noted in Appendix A, with the lateral addition of heat from a wall through heat transfer, the less computing time advantage is not gained because of the additional complexity of coordinating the fixed wall segments of heat exchangers with the variable fluid temperature wave fronts. However, in most power plant transient performance models, there are few heat exchangers, like superheaters; most heat additions can be direct, like boiling.

In the Appendix A, the continuity wave equation, its general solution, and the wave movement sequence used in all computer models, are presented. In Section 2, wave equations for one-dimensional single phase flow with wall heat transfer are presented; these are applied to a counter flow heat exchanger computer model in Section 3 and a transient example is shown. In Section 4, wave equations for one-dimensional two-phase flow with boiling are presented; and in Section 5, exact solutions to other first order differential equations, the second advanced method, are shown. These both are applied to a simplified model of the Advanced Boiling Water Reactor (ABWR) in Section 6, including two transient examples. Conclusions are drawn in Section 7.

Based on the first author’s TI 89 computer programs, the first coauthor prepared matlab versions, and performed the computer studies reported in this paper. This was part of a larger body of work done for his Master’s Degree Thesis [2], under the direction of the final coauthor.

2 Wave Equations for One-dimensional Single Phase Flow with Wall Heat Transfer

The basic differential equation for temperature in one-dimensional single phase flow with wall heat transfer, from Appendix A, and the differential equation for wall tempera-

ture are

$$\frac{\partial T}{\partial t} + V \frac{\partial T}{\partial x} = \frac{(T_w - T)}{\tau_f} \quad (1)$$

$$\tau_w \frac{\partial T_w}{\partial t} = T_a - T_w \quad (2)$$

where T is the fluid temperature ($^{\circ}\text{F}$), x is the distance (ft) along the pipe, V is the fluid and wave velocity at time t (sec), T_w is the average temperature of pipe section ΔL long, T_a is the average temperature of the fluid along ΔL , τ (sec) = $C'/(h * P)$, where C' (Btu/ft $^{\circ}\text{F}$) = $C_p * \rho * AF$ and h (Btu/secft ^2F) is the heat transfer coefficient (fluid-wall); P (ft) is the perimeter at pipe ID; C_p (Btu/lbF) is the heat capacity; ρ (lb/ft 3) is the density; AF (ft 2) is the flow area (fluid), cross section area (pipe). Note that $h = 1/(1/h_f + 1/h_w)$, where h_f is the fluid film coefficient and h_w is the pipe wall surface layer coefficient. Although V , T_w and T_a can vary with time; they are constant over time interval Δt .

The exact basic solutions for T after time interval Δt are

$$T = T_{wo} \left[1 - e^{(-\Delta t/\tau_f)} \right] + T_o e^{(-\Delta t/\tau_f)} \quad (3)$$

$$T_w = T_a \left[1 - e^{(-\Delta t/\tau_w)} \right] + T_{wo} e^{(-\Delta t/\tau_w)} \quad (4)$$

where the subscript 'o' represents a value at the previous time interval. T_o is also the final value of the upstream wave.

For no change of wave front in ΔL , at constant time t , the average fluid temperature, T_a , is

$$T_a = \left[\frac{T_1 - T_0 e^{(-\Delta L/l_f)}}{1 - e^{(-\Delta L/l_f)}} \right] - (T_1 - T_0) \frac{l_f}{\Delta L} \quad (5)$$

where, T_1 is the temperature at $x = \Delta L$, T_0 is the temperature at $x = 0$ and $l_f = V * \tau_f$. Change to a different T wave within ΔL is accounted for when calculating T_a in the computer models.

3 Counter Flow Heat Exchanger

3.1 Computer Model

Figure 1 is a schematic diagram of a counter flow heat exchanger (straight tube type [3]). From the last Section, Equation (3), the exact solution equations used for the transient performance of this heat exchanger are

Primary side waves:

$$T_p = T_{wpo} \left[1 - e^{(-\Delta t/\tau_p)} \right] + T_{po} e^{(-\Delta t/\tau_p)} \quad (6)$$

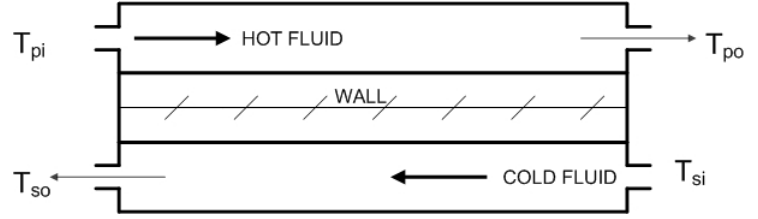


Fig. 1. Counter flow heat exchanger

Secondary side waves:

$$T_s = T_{wso} \left[1 - e^{(-\Delta t/\tau_s)} \right] + T_{so} e^{(-\Delta t/\tau_s)} \quad (7)$$

Wall:

$$T_w = \tau_w \left[\frac{T_{ap}}{\tau_{wp}} + \frac{T_{as}}{\tau_{ws}} \right] \left[1 - e^{(-\Delta t/\tau_w)} \right] + T_{wo} e^{(-\Delta t/\tau_w)} \quad (8)$$

where the subscript 'o' represents the value at previous time interval.

There are 2 average wall section 'surface' temperatures, T_{wf} , which are

$$T_{ws} = T_{wso} + (T_w - T_{wo}) \quad (9)$$

$$T_{wp} = T_{wpo} + (T_w - T_{wo}) \quad (10)$$

The wall thermal center, for T_w , is $(\tau_w/\tau_{ws}) * tw$ from the secondary side wall surface, where tw is the wall thickness. If $hp \approx hs$ then, $\tau_{wp} = \tau_{ws} = 2\tau_w$, and the thermal center is at $tw/2$.

The use of T_{wp} and T_{ws} adds an extra degree of freedom to T_w , effectively allowing a linear slope through tw . For output display only, at wall inlet and outlet, T_w is the linear extension from the nearest 2 values of calculated T_w . For heat transfer, the average temperatures of the primary fluid (T_{ap}) and secondary fluid (T_{as}), over $\Delta L = 0.2 L$ are used every Δt .

The computer model, HEATX, initiates in steady state. The overall heat transfer coefficient, U (Btu/ft 2 $^{\circ}\text{F}$ sec), is

$$U = 1/((1/hp) + (1/hs)) \text{ and in steady state}$$

$$Q = U * AHT * LMTD$$

where AHT is the heat transfer area and $LMTD$ is the log mean temperature difference, which is

$$LMTD = \frac{(T_{pi} - T_{so}) - (T_{po} - T_{si})}{\ln[(T_{pi} - T_{so})/(T_{po} - T_{si})]} \quad (11)$$

Also

$$Q = C'_p V_p (T_{pi} - T_{po}) = C'_s V_s (T_{so} - T_{si}) \quad (12)$$

3.2 Example Transient

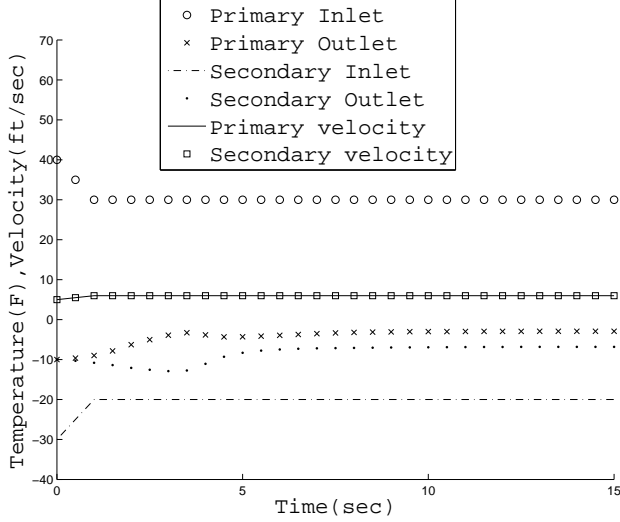


Fig. 2. Variations in Inlet and Outlet temperatures and Velocities vs Time

The model parameters and initial conditions are shown in Table 1. The transient is a very severe one, ramping the input variables in 1 second, and then holding them constant. Shown below are the transient changes induced to the initial conditions.

$$\begin{aligned} T_{pi} &: 40 \rightarrow 30(^{\circ}\text{F}) \\ T_{si} &: -30 \rightarrow -20(^{\circ}\text{F}) \\ V_p &: 5 \rightarrow 6(\text{ft}/\text{sec}) \\ V_s &: 5 \rightarrow 6(\text{ft}/\text{sec}) \end{aligned}$$

The time interval used is large: $\Delta t = 0.5$ sec. Figure 2 shows the inlet and outlet temperatures and velocities vs time. Figure 3 displays the heat flow, Q , across the wall vs time. Figures 4 shown in the next page illustrates very clearly the passage of the temperature waves through the length of the heat exchanger at times of 0, 1, 2, 3 and 5 seconds. After 15 seconds, the heat transferred out of the primary side equals the heat transferred into the secondary side to within $< 0.2\%$.

4 Wave Equations for One-dimensional Two Phase Flow with Boiling

The continuity equations for saturated steam and water, with change of phase [1], [4] are,

$$\frac{\partial \alpha}{\partial t} + \frac{\partial(\alpha V_g)}{\partial z} = \frac{\Gamma_g}{\rho_g} \quad (13)$$

Table 1. Model parameters and Initial conditions for HEATX

Length, L	20 (ft)
Heat transfer area, AHT	10000 ft^2
Overall heat transfer coefficient, U	550 ($\text{Btu}/\text{ft}^2 \text{ hr } ^{\circ}\text{F}$)
Total heat flow, Q	50 (k Btu/sec)
Primary side fluid	
Heat transfer coefficient, h_p	792 ($\text{Btu}/\text{ft}^2 \text{ hr } ^{\circ}\text{F}$)
Heat capacity/length	200 ($\text{Btu}/\text{ft } ^{\circ}\text{F}$)
Heat transfer time constant/Attenuation length	1.82 (sec)/9.1 (ft)
Velocity	5 (ft/sec)
Inlet/outlet temperature, T_{pi}/T_{po}	40/-10 ($^{\circ}\text{F}$)
Secondary side fluid	
Heat transfer coefficient, h_s	1800 ($\text{Btu}/\text{ft}^2 \text{ hr } ^{\circ}\text{F}$)
Heat capacity/length	500 ($\text{Btu}/\text{ft } ^{\circ}\text{F}$)
Heat transfer time constant/Attenuation length	2 (sec)/10 (ft)
Velocity	5 (ft/sec)
Inlet/outlet temperature, T_{si}/T_{so}	-30/-10 ($^{\circ}\text{F}$)
Wall	
Effective heat transfer time constant, τ_w	0.278 (sec)
Primary/secondary time constant, τ_{wp}/τ_{ws}	0.91 /0.4 (sec)

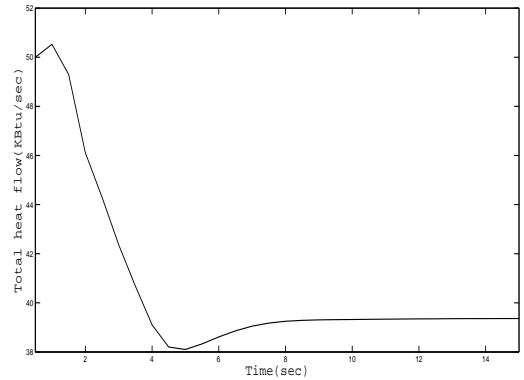


Fig. 3. Heat flow, Q across the wall vs Time

$$-\frac{\partial \alpha}{\partial t} + \frac{\partial([1 - \alpha] V_f)}{\partial z} = -\frac{\Gamma_g}{\rho_f} \quad (14)$$

where, α is the steam void fraction (–) which is the steam flow area/total flow area, V_g is the steam velocity (ft/sec), ρ_g is the steam density (lb/ft^3), V_f is the water velocity (ft/sec), ρ_f is the water density (lb/ft^3), and Γ_g is the steam generation rate ($\text{lb}/\text{ft}^3 \text{ sec}$) which is proportional to heat added to the mixture.

The Zuber-Findlay (Z-F) drift flux steam void fraction

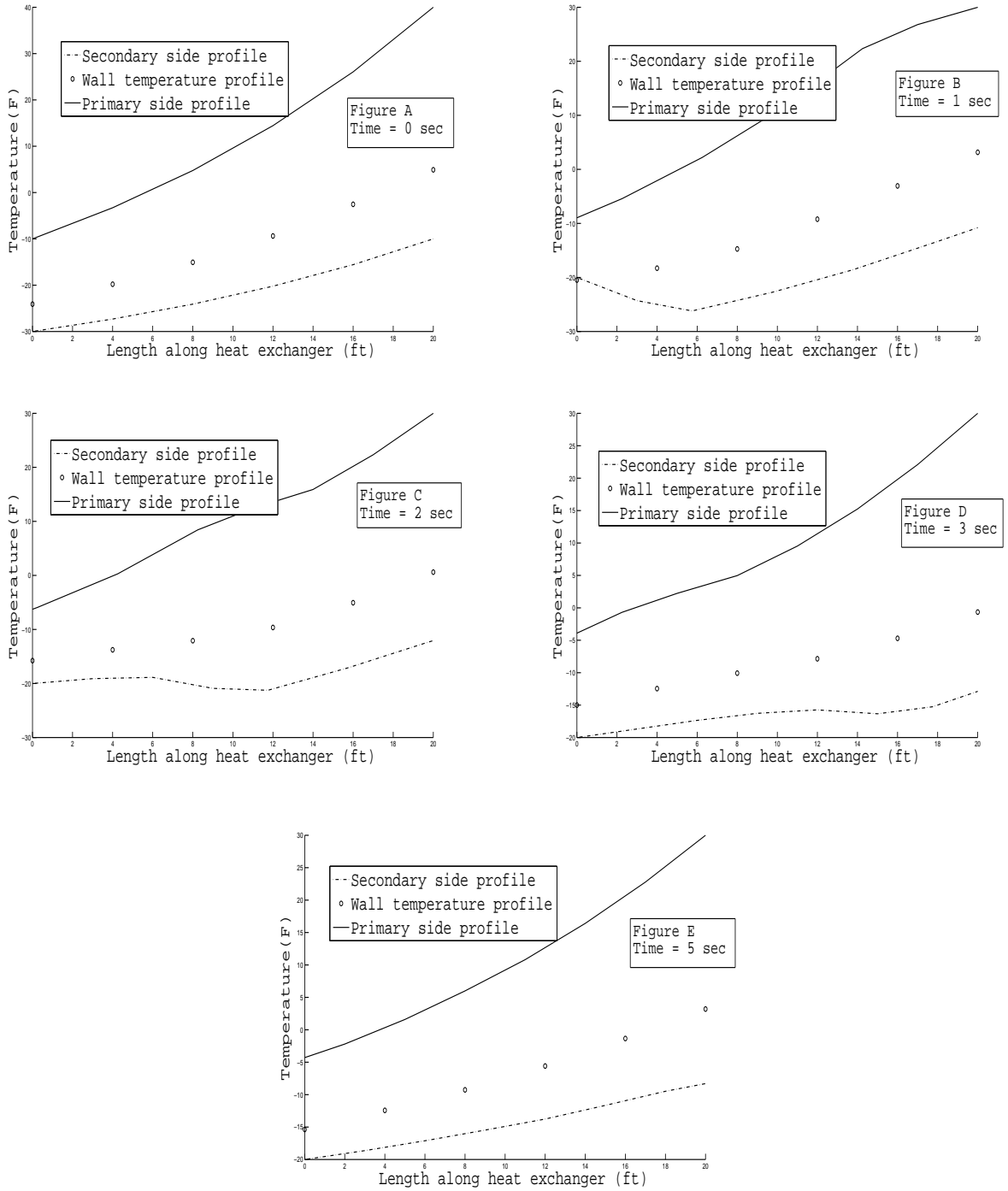


Fig. 4. Figures A to E show the temperature profile of the primary, secondary and wall through the length of the heat exchanger at time = 0,1,2,3 and 5 sec respectively.

model [5] is

$$V_g = \frac{J_m}{K_B} + V_d \quad (15)$$

where J_m is the mixture volumetric flux (ft/sec) which is $\alpha V_g + (1 - \alpha) V_f$, V_d is the vertical steam drift flux (ft/sec)

and K_B is the Bankoff void model constant [6] which is $1/C_o$, from Z-F.

Adding (13) and (14) we get,

$$\frac{\partial J_m}{\partial z} = (\Gamma_g / \rho_g) * p = (\Gamma_g / \rho_g)(1 - q) \quad (16)$$

where, $p = 1 - \rho_g/\rho_f = 1 - q$ and $q = \rho_g/\rho_f = 1 - p$. Then, integrating $\partial J_m/\partial z$ we get

$$J_m = [\Gamma_g/\rho_g] * p * [z - z_b - V_t t] + V_{f0} \quad (17)$$

where V_{f0} (ft/sec) is the water velocity at the boiling boundary, z_b (where boiling begins and $\alpha = 0$) and V_t (ft/sec) is the velocity of boiling boundary, z_b . Combining V_g and J_m in Z-F gives the steam velocity,

$$V_g = \frac{\Gamma_g * p}{\rho_g * K_B} * (z - z_b - V_t * t) + V_{f0}/K_B + V_d \quad (18)$$

Note that V_g , which is also the wave velocity, is directly proportional to Γ_g and z . Finally, substituting V_g into (13) yields:

$$\frac{\partial \alpha}{\partial t} + V_g * \frac{\partial \alpha}{\partial z} = \frac{\Gamma_g}{\rho_g} (1 - p * \alpha / K_B) \quad (19)$$

This is the continuity wave equation for α , corresponding to the first equation in Appendix A. Following the method outlined in Appendix A, the exact solutions to this equation, for Γ_g constant with z and Δt , and including boundary conditions, are

$$z_v = z_o + \left[\frac{z_o - z_b + (V_{f0}/K_B + V_d - V_t)(\rho_g K_B)}{(\Gamma_g * p) \left[e^{\left[\frac{\Gamma_g * p}{\rho_g * K_B} \Delta t \right]} - 1 \right]} \right] + V_t \Delta t \quad (20)$$

$$\alpha_v = \frac{K_B}{p} \left[1 - [1 - \alpha_o(p/K_B)] e^{-\left[\frac{\Gamma_g * p}{\rho_g * K_B} \Delta t \right]} \right] \quad (21)$$

where z_v is the wave front at Δt , α_v is α at z_v , the subscript 'o' is the value at the previous time. These are the wave equations used for boiling flow in the heating channel of the ABWR model in Section 6.

5 Exact Solutions to Other First Order Differential Equations

Among several exact solutions to first order differential equations used in the authors' computer studies, the major one is the response to a ramp input for a lead/lag control circuit with the transfer function,

$$\frac{Y}{X} = \frac{[1 + T_2 s]}{[1 + T_1 s]} \quad (22)$$

The exact solution used as a "function" in the computer programs is

$$Y = \left[\frac{(X - X_o)(T_2 - T_1)}{\Delta t} - (Y_o - X_o) \right] * (1 - e^{-\frac{\Delta t}{T_1}}) + Y_o + X - X_o \quad (23)$$

where the subscript 'o' is the value at previous time. A ramp is used as the best approximation to the variation of the input variable over the previous Δt , and it produces very little error. In the ABWR model, described in the next section, this function is used seven times, including the model for the steam turbine.

6 Advanced Boiling Water Reactor - ABWR

6.1 Computer Model

The ABWR model evolved from [7]; the improved pressure and water level models herein are based more on first principles, and the new heating channel model is described in Section 4.

The core reactivity, reactor kinetics, reactor power and channel heating are the same as [7], except for the omission of decay heat power. The remainder of the model is the same as [7], with some minor simplifications. Figures 5 through 10 show the major parts of the model in simplified block diagram form, and also show the symbols for the main variables, which are all per unit, except for the velocities and heights in the heating channel, per Section 4.

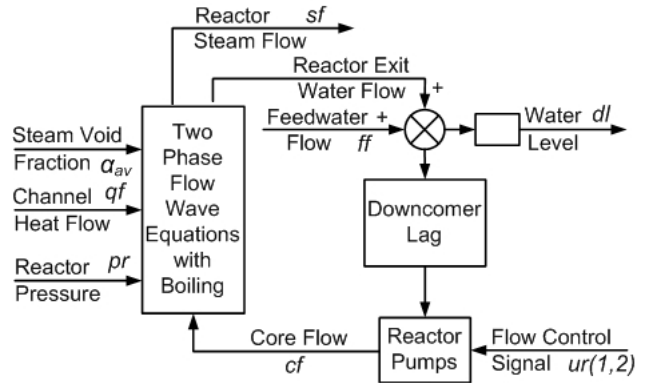


Fig. 5. Reactor flow heating channel and water level.

As shown in Figure 6 on the next page, there are 3 sources of reactivity change, Δk : control rods, core (average) steam void fraction, and channel heat flow (which is really fuel rod temperature, or Doppler effect). These 3 Δk 's combine algebraically to form "excess Δk ", which changes reactor power.

The multivariable control has been modified and simplified from [7], as follows:

$$vr * km = ur \quad (24)$$

where vr , km and ur are all matrices.

$$vr(1 \times 6) = [v_1 \ v_2 \ v_3 \ v_4 \ v_5 \ v_6] \quad (25)$$

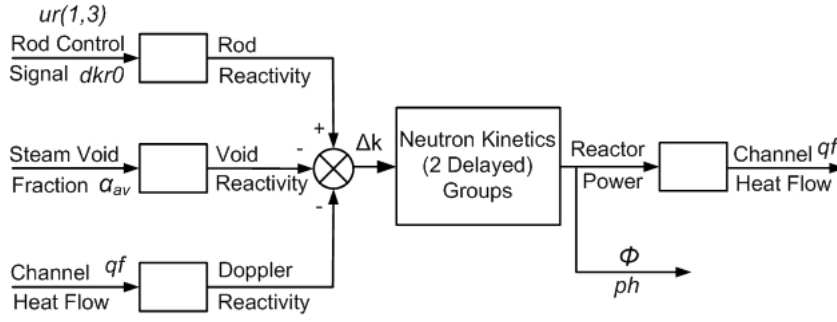


Fig. 6. Reactor Power and Heat Flow diagram, also showing the sources of reactivity change which are Rod, Void and Doppler reactivity.

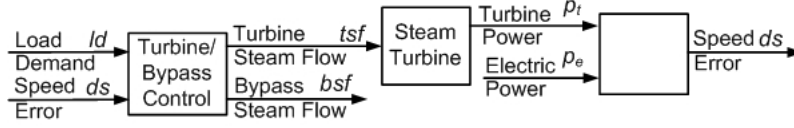


Fig. 7. Turbine and Bypass valve model

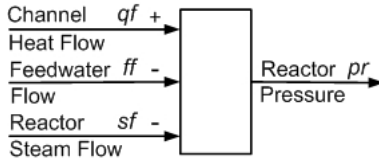


Fig. 8. Reactor pressure

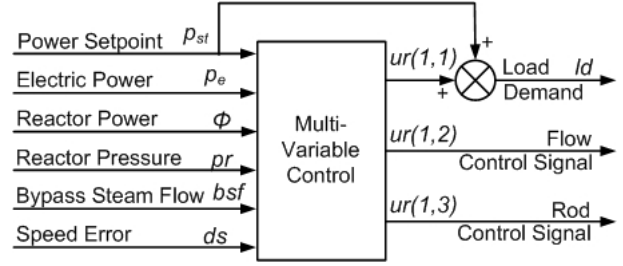


Fig. 10. Multivariable control model

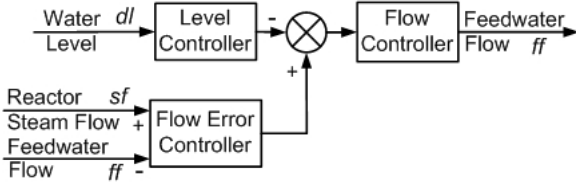


Fig. 9. Feedwater control

$$km = \begin{bmatrix} 1.0 & 0.4 & 1.0 \\ 0.3 & 0.0 & 0.3 \\ 0.0 & 0.2 & 1.0 \\ 0.0 & 0.1 & 0.5 \\ -1 & 4.0 & 20 \\ -0.3 & 0.3 & 1.0 \end{bmatrix} \quad (26)$$

$$ur(1 \times 3) = [u_1 \ u_2 \ u_3] \quad (27)$$

Also we have $v_1 = pst - pe - 20 * ds$, $v_2 = \int v_1 dt$, $v_3 = 0.5 bsf + pe - ph$, $v_4 = \int v_3 dt$, $v_5 = 1 - pr$ and $v_6 =$

$\int v_5 dt$ and also $pst + ur(1,1) = ld$, $cf0 + ur(1,2) = cf$ and $-0.002 - ur(1,3) = dkr0$.

Note that $ur(1,2)$ and $ur(1,3)$ are not used together, only one at a time. In normal steady state, v_1 , v_3 and v_5 are 0; v_2 , v_4 and v_6 are initialized at 0. Although modified, the same design process described in [7] was not used, and additional control tuning using the [7] design procedure should improve the ABWR model transient performance to a certain extent. Rated base values of the ABWR model are given in Table 2 shown in the next page.

Reactor power (Φ) is controlled by core flow (cf) between 100% and 70%, and by control rods (Δkr) between 70% and 50%, with automatic switchover in the model. At 70% power, reactor flow is 60.85%, and α_{av} is 42.02%; at 50% power, α_{av} is 35.91%, and control rods have been inserted for steady state $\Delta kr = -\$1.63$.

Figure 11 on the next page shows the calculated steady state profile of steam quality, $x(-)$, and void fraction, $\alpha(-)$, at full power, up the heating channel from the reactor core inlet to the core exit. Note the negative quality, perunit sub-cooling, from the core inlet to the elevation where boiling begins, z_b .

The boiling section variables were calculated with the exact solution wave model of Section 4; the preheat or sub-cooled section was calculated using the exact solution wave

Table 2. Base values of the ABWR Model

Reactor Power	3800 MW
Reactor Power Flow	31970 lb/sec
Reactor Steam/Feedwater Flow	4587 lb/sec
Reactor Steam Bypass System	30%
Turbine/Generator Power	1300 MW
Reactor Pressure	1000 psia
Reactor water level range	± 15 in
Core exit quality, x_{er}	14.35%
Core average void fraction, α_{avr}	40.98%
Core inlet subcooling, tor	-3.47%

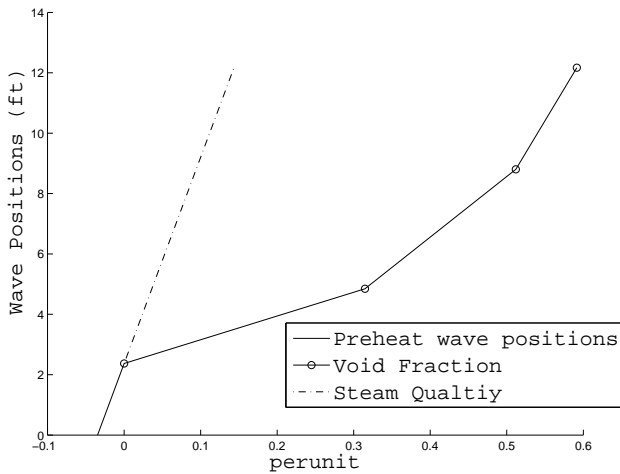


Fig. 11. Steady state profile of Steam quality, x and Void fraction, α through the heating channel

model of Section 2, but with direct heating of the water.

There are 2 types of transients that can be run with the ABWR model:

1. normal power maneuvering, 50% \leftrightarrow 100% power, and
2. partial load rejections (PLR's), 50% \leftrightarrow 100% power.

For normal power maneuvering, $p_e = p_t$ and $ds = 0$. While actual Power Set Point (p_{st}) rates are limited to 10% per minute (1% per 6 sec), double these rates can be used with the ABWR model. Note that control will automatically switch between flow and rods at 70% power. In the model, all $\Delta k'$'s are set at 0 for the initial power level. For PLR, a new p_e , less than the initial power by no more than 30%, is input and remains constant. Since $p_t > p_e$, ds increases and lively action ensues. After p_t settles out at p_e (usually < 30 sec), another transient segment can be run, restoring $p_{st} \rightarrow p_e$ (ds and bsf to 0). For the initial part of a PLR, a time interval of $\Delta t = 0.1$ sec should be used; otherwise a time interval of $\Delta t = 1/3$ sec is fine for all other transients.

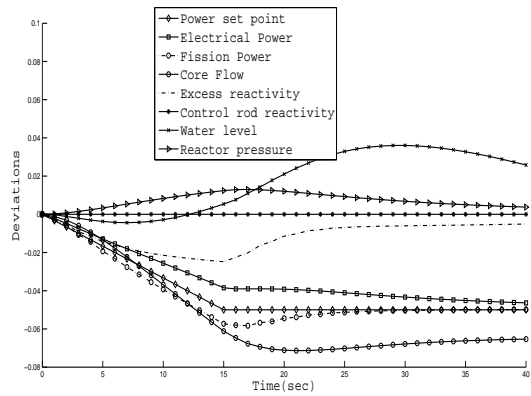


Fig. 12. ABWR maneuvering transient power change from 100% to 95% with a transient ramp time of 15 sec and the final time of 40 sec.

6.2 Example Transients

Figure 12 shows an ABWR maneuvering transient from 100% power to 95%, at the fast change rate of 1% for 3 sec. The model performs very smoothly with a Δt of 1/3 sec. The maximum water level deviation is only a very small 0.56 inches, 0.037 pu of the ± 15 inch range.

Figure 13 shows a partial load rejection from 100% to

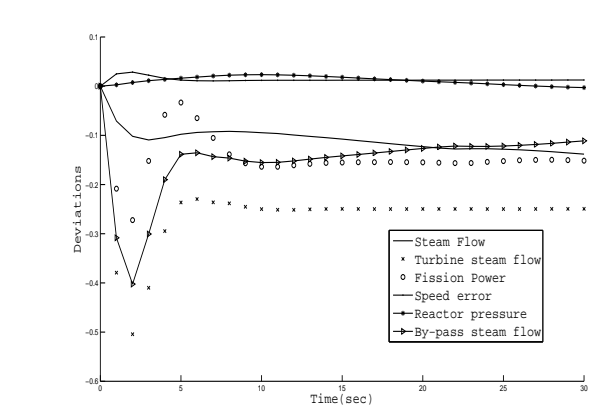
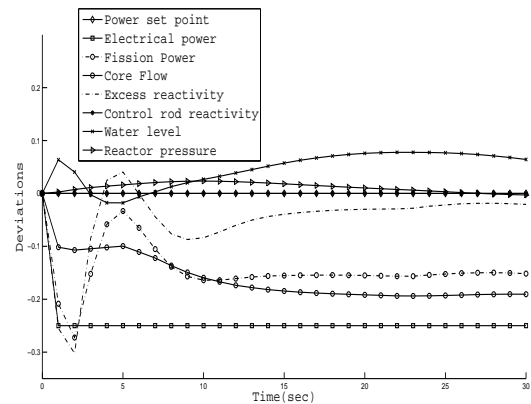


Fig. 13. ABWR maneuvering a PLR from 100% to 75% power with $\Delta t = 0.1$ sec for the first 10 seconds and $\Delta t = 1/3$ sec for the last 20 seconds.

75%. For the first 10 seconds, $\Delta t = 0.1$ sec because of the fast action; for the last 20 seconds, $\Delta t = 1/3$ sec for more normal transient behavior. Note that the negative of the bypass flow is shown to reduce plot space. The p_{st} remains at 100% throughout. The initial variations of turbine and bypass steam flow are large, showing the severity of the transient. The variations of reactor steam flow and reactor power are not as large, showing the value of the steam bypass system.

7 Conclusion

The major conclusion of this paper is that two advanced modeling methods have been successfully applied to computer models of a counterflow heat exchanger and the ABWR. The methods are:

1. 'continuity wave' equations for the transport of thermal energy through one dimensional flow paths;
2. the exact solution of differential equations analytically first, and then the solutions put into the program.

The advantages of these advanced methods were stated to be: greater accuracy with simplified models and less computing time, for most of the applications, because the exact solutions permit larger time intervals. Although no direct evidence has been presented in this paper to support these advantages, exact solutions are always the standard for evaluating numerical approximations and it is clear that larger time intervals require less computing time for similar calculations.

Computer Program Availability Matlab versions of HEATX and ABWR can be downloaded at: www.ecse.rpi.edu/homepages/chowj

References

- [1] Wallis, G. B., 1969. *One-Dimensional Two-Phase Flow*. McGraw-Hill.
- [2] Muralimanohar, P. K., 2008. "Advanced power plant modeling with applications to the advanced boiling water reactor and the heat exchanger". Master's thesis, Rensselaer Polytechnic Institute, December.
- [3] Bird, R. B., Stewart, W. E., and Lightfoot, E. N., 1962. *Transport Phenomena*. J. Wiley.
- [4] Zuber, N., and Staub, F. W., 1967. "An analytical investigation of transient response of volumetric concentration in a boiling forced-flow system". *Nuclear Science and Engineering*, **30**(2), pp. 268–278.
- [5] Zuber, N., and Findlay, J. A., 1965. "Average volumetric concentration in 2-phase flow systems". *Journal of Heat Transfer*, **87**, pp. 453–468.
- [6] Bankoff, S. G., 1960. "A variable density single fluid model for two-phase flow with particular reference to Steam-Water flow". *Journal of Heat Transfer*, **82**, p. 265.
- [7] Younkins, T. D., Winkelman, J. R., Sanchez-Gasca, J. J., and McGrady, J. A., 1987. "Output feedback multi-variable control for an advanced boiling water reactor". *Transactions on Energy Conversion*, **EC-2**.
- [8] Hildebrand, F. B., 1949. *Advanced Calculus for Engineers*. Prentice-Hall.

Appendix A: Wave Equation Solutions and Computer Model Wave Movement Sequences

The "continuity" wave equation in one spatial dimension has one unknown, or dependant variable, Y , and two independent variables, t (sec) and x (ft), and is given as

$$\frac{\partial Y}{\partial t} + V * \frac{\partial Y}{\partial x} = Q \quad (28)$$

where, in general we have $V = V(x, t)$. The flow velocity V is also the wave speed.

There are two solutions to this wave equation, which can be broken down into two ordinary differential equations, as follows [8]

$$dt = dx/V = dY/Q = \text{constant}, \quad (29)$$

because dt , dx and dY are arbitrary. Then from dt and dx we have

$$dx/dt = V \quad (30)$$

with solution

$$\int V * dt = \Delta X_{vi} \quad (31)$$

where ΔX_{vi} is the change in wavefront or wave position and $\Delta X_{vi} = X_{vi} - X_{vi0}$, where X_{vi0} is the initial value of X_{vi} at $t - \Delta t$ and i is the wave number.

Then from dt and dY we have

$$dY/dt = Q \quad (32)$$

with solution

$$\int Q * dt = \Delta Y_{vi} \quad (33)$$

where ΔY_{vi} is the change in Y corresponding to ΔX_{vi} and $\Delta Y_{vi} = Y_{vi} - Y_{vi0}$.

In addition, a third dependent ordinary differential equation can be written from dx and dY which is

$$dY/dx = Q/V \quad (34)$$

The solution to this equation is

$$\int (Q/V) * dx = Y(X_1) - Y(X_0) \quad (35)$$

Equation (35) is used to obtain the variation of Y with x at a constant t , where $X_1 = X_{vi}$ at time t and $X_0 = X_{vi-1}$ at time t .

The computer models in this paper use the same basic method to sequence the movement of the waves from one set of positions to the next set of positions over time interval $\Delta t = dt$. Two primary lists (x_{vl}, y_{vl}) are used for X_v and corresponding Y_v . Additional lists may be used for other corresponding variables.

These lists are initialized with at least 2 values each, one at the inlet and the other at the exit of the flowpath. Other values within the flowpath are added at discrete intervals, or the two waves are advanced in “false time” until the wave at the inlet of the flowpath passes the exit of the flow path. Then this last wave is repositioned at the exit of the flowpath. The total number of waves is placed in index label “K”, which is a computer model variable.

At every value of time (t), a new wave starts at the inlet of the flowpath. The inlet value Y_i comes from elsewhere in the model, and is put into $y_{vl}[1]$ at the end of the wave movement sequence, which is described in the following paragraph.

At new time t , K is increased by 1, with nothing in $x_{vl}[\text{new } K]$ and $y_{vl}[\text{new } K]$. Then the following do-loop is executed, starting at the exit of the flowpath and indexing down to wave position 2.

```
For i = K : -1 : 2
  j = i - 1
   $x_{vl}[i] = x_{vl}[j] + \Delta X_v$ 
   $y_{vl}[i] = y_{vl}[j] + \Delta Y_v$ 
End For
```

Note that no essential information is lost or overwritten. Also, the number of each wave increases by one for each Δt , as the wave progresses through the flow channel. $x_{vl}[1]$ remains the same at the inlet of flowpath. A new value of inlet Y_i is put into $y_{vl}[1]$. Another do-loop then sets K such that there is one value of X_v at or beyond the exit, X_e . The exit value of Y is found by using the foregoing solution to the third differential equation, where $X_{vi} = X_e$.

If Q is constant with x , changing only with a new Δt , as with uniform heating along the flow channel, then comparisons show that the basic wave solution computer model is more accurate and faster than comparable fixed spatial coordinate (Euler type) models, because the exact wave solutions permit larger time intervals.

If the value of Q changes over n sections of Δx , between inlet and exit, then at least two more lists for Q and ‘ Q position’ are required. Q is obtained for each wave and part wave in a separate do-loop that accounts for the proper Δx ’s and part Δx ’s between the 2 waves. This separate do-loop is inside the foregoing wave movement loop. Heat transfer between the wall and fluid requires another two lists for average section temperature of the wall and fluid. An additional do-loop calculates these average temperatures for the next time (t), after the wave position loop. Although the additional lists and do-loops complicate the basic wave solution computer model, it is still more accurate, but no faster than the Euler type models.